conditions. For this reason, equilibrium CCN concentrations may often not be realized in nature. For example, marine boundary layer clouds that form in air with high CCN concentrations should retain high droplet concentrations for several days, provided that the microphysics of the cloud is determined by the CCN concentration rather than changing boundary conditions.

Residence times are another useful measure of CCN lifetimes. The residence time (τ) is equal to the equilibrium concentration of a quantity divided by its production rate. Using our results, the residence times for CCN number concentration (τ_N) and mass concentration (τ_M) are shown in Fig. 3. The three-day relaxation of N from an initial value of 1,100 cm^{-3} to its equilibrium value of 250 cm^{-3} (Fig. 1) is consistent with an e-folding time of one day, which is close to the values shown in Fig. 3.

Because many processes that reduce CCN number concentrations do not affect CCN mass concentrations, τ_M always exceeds τ_N. As these two residence times can differ so much (Fig. 3), it is important to distinguish between them when estimating the effects of aerosols on cloud properties.

At low CCN concentrations, the deposition of drizzle on the ocean is the dominant sink for CCN mass, whereas the coalescence of cloud droplets is the dominant sink for CCN numbers. At high CCN concentrations, as the removal of CCN mass by drizzle reaching the ocean gradually becomes insignificant, τ_M is controlled by the dry deposition of CCN to the ocean. For CCN deposition velocities, we use the formulation of Giorgi[10], in which the deposition velocity is a minimum (~0.01 cm s^{-1}) for particles of radius ~0.1 μm. Because CCN deposition velocities are uncertain, we ran an additional simulation in which the minimum value of the deposition velocity was 0.1 cm s^{-1}. This reduced our calculated value of τ_M by ~25%, as shown in Fig. 3, but had negligible effect on τ_N.

Although we find no evidence of a bistability in the steady-state relation between CCN concentrations (N) and source strength (S_0), we agree with BC that N is strongly dependent on S_0. Accordingly, there is a significant potential for changes in CCN production rates to change cloud droplet size distributions, cloud albedo, and therefore, climate. We find, however, it can take several days for N to reach equilibrium values. Therefore, clouds should be more sensitive to the highest CCN concentrations to which they are exposed than to the CCN production rates in regions to which they may be advected. □

Received 9 November; accepted 9 December 1993.

1. Twomey, S., Piepgrass, A. M. & Wolfe, T. L. *Tellus* **36B,** 356–366 (1984).
2. Baker, M. B. & Charlson, R. J. *Nature* **345,** 142–145 (1990).
3. Ackerman, A. S., Toon, O. B. & Hobbs, P. V. *J. atmos. Sci.* (Submitted).
4. Toon, O. B., Turco, R. P., Westphal, D., Malone, R. & Liu, M. S. *J. atmos. Sci.* **45,** 2123–2143 (1988).
5. Duynkerke, P. G. & Driedonks, A. G. M. *J. atmos. Sci.* **44,** 43–64 (1987).
6. Toon, O. B., McKay, C. P., Ackerman, T. P. & Santhanam, K. *J. geophys. Res.* **94,** 16287–16301 (1989).
7. Nicholls, S. *Q. Jl. met. Soc.* **110,** 783–820 (1984).
8. Nicholls, S. & Leighton J. *Q. Jl. met. Soc.* **112,** 431–460 (1986).
9. Ackerman, A. S., Toon, O. B. & Hobbs, P. V. *Science* **262,** 226–229 (1993).
10. Giorgi, F. *J. geophys. Res.* **91,** 9794–9806 (1986).

ACKNOWLEDGMENTS. This work was supported by NASA, the US DOE, the US ONR and the US NSF. We thank M. Baker and R. Charlson for discussions.

Rapid interglacial climate fluctuations driven by North Atlantic ocean circulation

Andrew J. Weaver & Tertia M. C. Hughes

School of Earth and Ocean Sciences, University of Victoria, PO Box 1700, Victoria, British Columbia V8W 2Y2, Canada

RECENT data from the GRIP ice core[1–3] in Greenland suggest that the climate of the last (Eemian) interglacial period was much less stable than that of the present interglacial. Rapid transitions between warm and cold periods were found to occur on timescales of just a few decades. The North Atlantic climate during the Eemian period was also shown to be characterized by three states, respectively warmer than, similar to and colder than today[1,2]. Recent data from the nearby GISP2 ice core have revealed some discrepancies with these findings, which remain to be resolved[4,5]. Here we present simulations using an idealized global ocean model, which suggest that the North Atlantic ocean has three distinct circulation modes, each of which corresponds to a distinct climate state. We find that adding a simple random component to the mean freshwater flux (which forces circulation) can induce rapid transitions between these three modes. We suggest that increased variability in the hydrological cycle associated with the warmer Eemian climate could have caused transition between these distinct modes in the North Atlantic circulation, which may in turn account for the apparent rapid variability of the Eemian climate.

One of the most important indicators of past climates and their variability is the record from the Greenland ice cores. Early analyses of these ice cores have shown that the climate of the North Atlantic during the last glaciation was marked by abrupt swings between relatively warm and relatively cold regimes[6–8]. These climate shifts were observed to occur very rapidly (over several decades) and quite frequently (every several thousand years or so). Similar oscillations have been found during the transition between the glacial and interglacial climates, the most recent of which was the Younger Dryas event which ended ~10,000 yr ago[9–11]. Although it has long been known that the climate of our present Holocene period has been marked by much weaker natural climate variability on both the century[12] and decadal[13] timescales, we have not observed any rapid and dramatic climate shifts.

The Greenland Ice-core Project (GRIP) 3028.8-m ice core from Summit, Greenland[1,2] provides high-resolution climatic information through the Eemian and into the penultimate glaciation. The Greenland Ice Sheet Project 2 (GISP2) recently reported results from a 3,053.4 m core drilled 28 km to the west of the GRIP core[4,5]. Although the two cores correlated extremely well over the top 90% of the record, the correlation in the rest

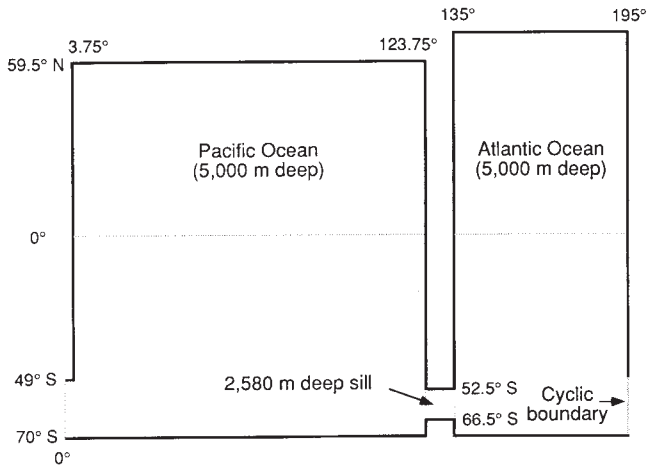

FIG. 1 The geometry (plan view) of the idealized two-basin model used in this study. All longitudes are measured relative to the western boundary of the model domain.

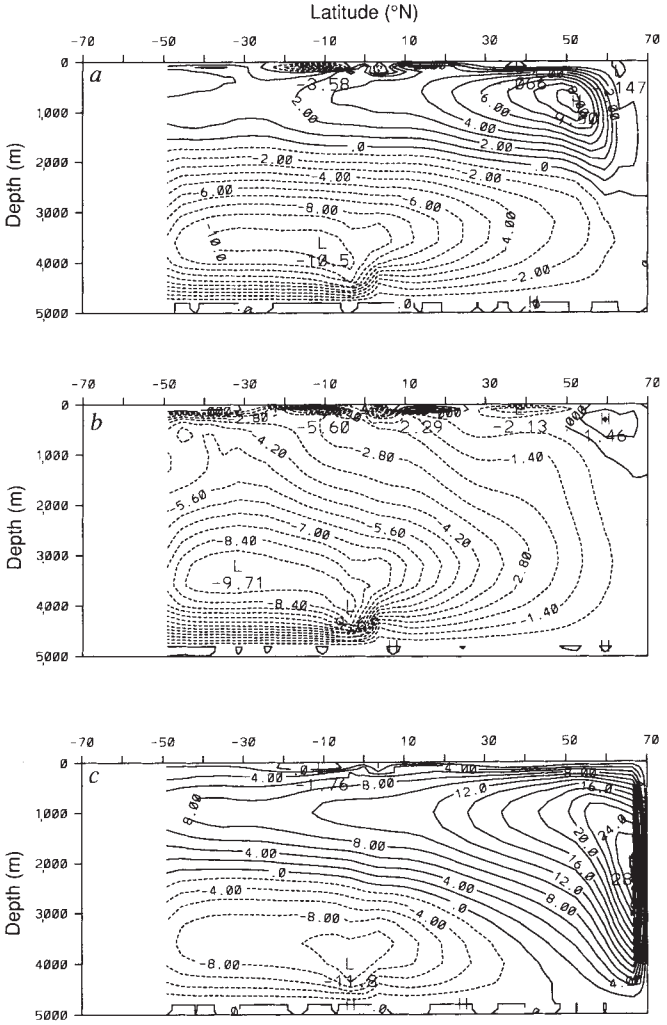

FIG. 2 The Atlantic Ocean meridional overturning streamfunction in Sv (1 Sv is 10^6 m^3 s^{-1}) for the three equilibria. *a*, The normal 'present-day' conveyor. *b*, The weak 'colder' conveyor. *c*, The strong 'warmer' conveyor. The *x*-axis is the latitude with positive and negative values indicating °N and °S, respectively. Positive and negative contours indicate clockwise and counterclockwise circulations, respectively, with H and L indicating local maxima and minima, respectively.

of the core, including the Eemian, was poor[5]. Several reasons (most probably related to flow deformation at one or both of the core sites) for this poor correlation were discussed in refs 4 and 5. Nevertheless, it has been reported[1,5] that over the first 2,847 m (~129,000 yr) of the GRIP core, which includes most of the Eemian (~115,000–135,000 yr ago), there was no significant disturbance of the ice layering. Such disturbances were first observed at a depth of 2,678 m in the GISP2 core (well above the component of the core associated with the Eemian). Although the initial ice analysis suggests that "the GRIP record can be interpreted climatically to a greater depth than the GISP2 record"[5], we must await more detailed ice-core analysis to confirm the GRIP findings. We suggest here that our model results are, however, consistent with the GRIP findings.

Previous theories of the glacial millennial-timescale oscillations have involved an interaction between continental ice sheets, the Atlantic-to-Pacific hydrological cycle and the thermohaline circulation of the North Atlantic[14]. It has further been proposed that the Younger Dryas event was just one such cycle modified by the division of melt water from the Mississippi to the St. Lawrence[15]. These theories cannot apply to the Eemian period as the large-scale continental ice sheets were not in existence then. Here we suggest that the fluctuations of the ocean's thermohaline circulation can alone explain such rapid climate shifts.

We use an idealized (Fig. 1) ocean general circulation model (OGCM)[16] forced by idealized steady winds[17]. For economy of calculation we use coarse horizontal resolution (3.75° meridional × 3.5° zonal) with 19 vertical levels varying from 50-m grid box thickness near the surface to 420-m grid box thickness near the bottom. The model was initially integrated for 3,288 yr to equilibrium by relaxing the surface temperatures and salinities of the ocean to observed zonally-averaged Pacific and Atlantic values[18] with a timescale of 50 d.

On reaching the 'present-day' climatological equilibrium under the relaxation boundary conditions, the amount of fresh water into and out of each surface grid box was determined. This diagnosed flux was then used as a specified boundary condition on salinity, while the thermal boundary condition was left unchanged (known as mixed boundary conditions; see, for example, ref. 19) for all further integrations. In the absence of a fully prognostic atmospheric model, mixed boundary conditions are often used to reflect the fundamental difference in evaporation–precipitation and thermal coupling between the ocean and the atmosphere.

The 'present-day' climatology was perturbed many times in an attempt to determine all possible equilibria of the idealized system. This exhaustive procedure yielded only three different configurations for the North Atlantic conveyor[20]. Figure 2 illus-

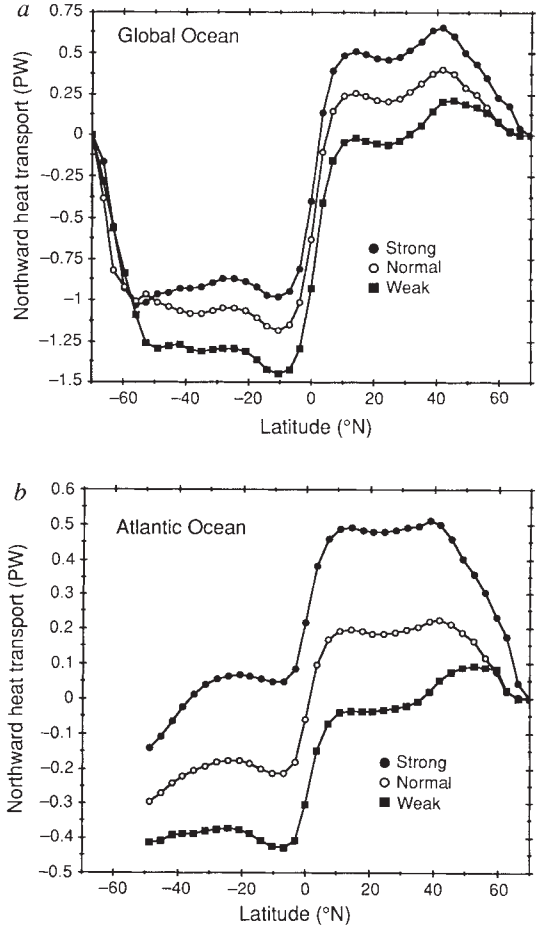

FIG. 3 The poleward heat transport in PW (1 PW is 10^{15} W) associated with the three equilibria portrayed in Fig. 2. *a*, The global ocean (Pacific + Atlantic + Southern oceans). *b*, The Atlantic Ocean only.

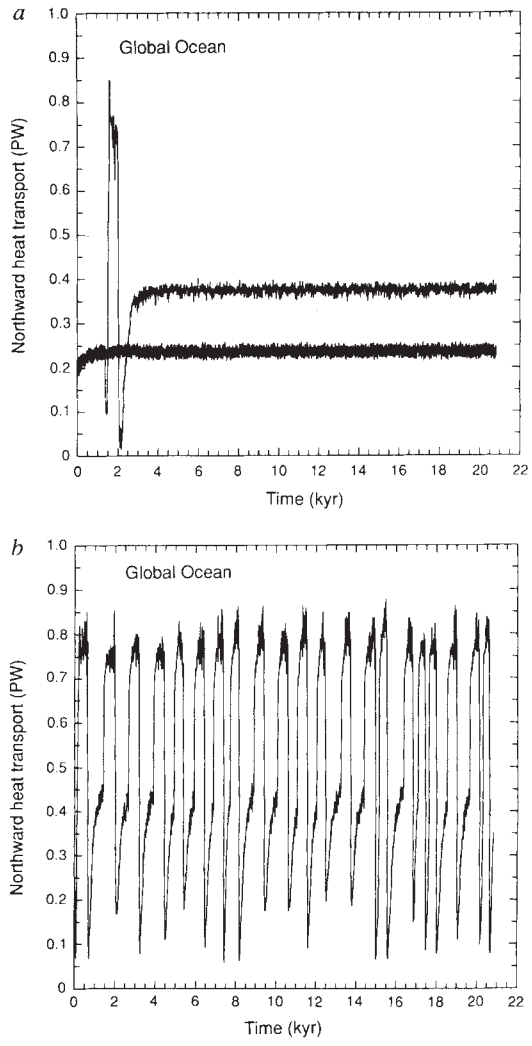

FIG. 4 The global ocean poleward heat transport at 28° N over the 20,800 yr of integration. *a*, The weak stochastic experiment (standard deviation, s.d. = 16 mm per month, lower curve) and the medium stochastic experiment (s.d. = 32 mm per month, upper curve). *b*, The strong stochastic experiment (s.d. = 48 mm per month).

trates these three different equilibria. In the first (Fig. 2*a*) the conveyor has a moderate 'present-day' strength of ~10–12 Sv (1 Sv is 10^6 m^3 s^{-1}). The other equilibria correspond to a weakened ('colder'—Fig. 2*b*) and an enhanced ('warmer'—Fig. 2*c*) conveyor. We were not able to induce a stable equilibrium with North Pacific sinking. Indeed, in all three configurations of the Atlantic conveyor, the Pacific Ocean remained virtually unchanged.

The poleward heat transport in the global ocean and in the North Atlantic associated with the three equilibria are shown in Fig. 3*a* and *b*, respectively. In the 'present day' (normal) climate ~0.2 PW (1 PW is 10^{15} W) is transported northward at 28° N. This increases to 0.5 PW in the 'warmer' climate case associated with an intensified North Atlantic thermohaline circulation, and decreases to −0.03 PW in the 'colder' climate. The zonally-averaged North Atlantic oceanic surface heat flux, $Q(y)$, (where y is positive northwards) can be determined from these equilibrium heat transports, $T(y)$, as $dT/dy = Q(y)$. Hence the three equilibria correspond to normal, enhanced and decreased ocean-to-atmosphere heat fluxes in the North Atlantic ocean and hence, one would expect, normal, warmer and colder North Atlantic sea surface temperatures and climates, respectively.

The stability of the present-day climatic state (Fig. 2*a*) was then tested by adding a stochastic component with varying magnitude to the freshwater flux forcing field as in ref. 21. This procedure was adopted as a simulation of high-frequency atmosphere variability[22]. Four experiments were carried out with the standard deviation (s.d.) of the stochastic component being set to 16, 32, 48 or 64 mm per month corresponding to 20, 40, 60 and 80% of the globally-averaged annual mean precipitation[23,24]. As the Eemian interglacial was, on average, slightly warmer than today[3], we interpret the high-s.d. experiments as a representation of an enhanced hydrological cycle associated with the warmer climate. Recent coupled atmosphere–ocean simulations[25] of the climatic response to increasing atmospheric CO_2 have noted that the hydrological cycle intensifies as the climate warms, and hence our representation is quite reasonable.

When only a weak (s.d. = 16 mm per month) stochastic forcing was used, the 'present-day' overturning (Fig. 2*a*) remained largely unchanged (Fig. 4*a*). A Fourier spectrum of the curve shown in Fig. 4*a* revealed variability with peaks at both decadal and century timescales, linked to horizontal and overturning advective timescales, respectively[21]. When the stochastic forcing was increased to s.d. = 32 mm per month, the 'present-day' climate remained stable for ~1,000 yr, when the conveyor in the North Atlantic suddenly collapsed (to a state similar to Fig. 2*b*), then increased rapidly, collapsed again and then settled into the new 'warmer' climatic equilibrium (as in Fig. 2*c*). Superimposed on this climatic equilibrium was variability on both decadal and century timescales. In the s.d. = 48 mm per month integration (Fig. 4*b*) the system oscillated internally between states involving weak (minima in Fig. 4*b*) and strong (maxima in Fig. 4*b*) overturnings in the North Atlantic, passing through a period of normal (middle state in Fig. 4*b*) overturning along the way. The partitioning of time in each state is similar to that observed in the Eemian (Fig. 3 in ref. 1). At no time during any of the integrations was deep water formation found to occur in the Pacific Ocean. The transition between the states happened very rapidly (over several decades) and the system remained in a particular state for periods up to a thousand years or so. Once more, superimposed on the millennial-timescale variability was variability on both decadal and century timescales. The results of the final experiment (s.d. = 64 mm per month) were similar to those of the s.d. = 48 mm per month experiment, except that the frequency of catastrophic transitions increased and their magnitude decreased, consistent with the idealized single-basin study of ref. 21.

Although the model used here is idealized and so should be viewed as process-oriented rather than predictive, its results are significant because they suggest that climate variability during the last interglacial (which has been found in the GRIP ice-core data) may be due to fluctuations of the ocean's thermohaline circulation. Unlike previous theories of rapid climate fluctuations during glacial periods and during the transition between glacial and interglacial periods, our experiments did not involve continental ice/runoff–ocean interactions or major modifications of the Atlantic-to-Pacific hydrological cycle. One might speculate that such variability may well have also existed in glacial times although ice/runoff–ocean interactions must certainly be accounted for. For example, as shown in ref. 20, the occurrence of sudden ice-melt or freshwater run-off, or a modification of the hydrological cycle from the Atlantic to the Pacific Ocean, could indeed also induce transitions between equilibria consistent with these earlier theories and model results (for example, refs 26–29).

The stability of the 'present-day' model climate and associated weak decadal and century timescale variability under weak random forcing are also consistent with the observations in the present Holocene climate. Nevertheless, we are still left with the fundamental question of why the stability of our present Holocene would be different from that of the Eemian interglacial. We have suggested that the difference would be linked to an

enhanced hydrological cycle associated with the warmer[3] mean climate of the Eemian, represented here as an increase in the magnitude of stochastic component of the freshwater flux forcing. We further suggest that this enhanced hydrological cycle would excite fluctuations of the North Atlantic conveyor between different modes of operation. If the variability found in the GRIP ice-core data is corroborated, then the Eemian interglacial may offer us a glimpse of the type of rapid climate variability which we might expect in a future climate warmed by means of anthropogenic greenhouse gas emissions. □

Received 23 August; accepted 9 December 1993.

1. GRIP Project Members *Nature* **364,** 203–207 (1993).
2. Dansgaard, W. *et al. Nature* **364,** 218–220 (1993).
3. White, J. W. C. *Nature* **364,** 186 (1993).
4. Taylor, K. C. *et al. Nature* **366,** 549–552 (1993).
5. Grootes, P. M., Stuiver, M., White, J. W. C., Johnsen, S. & Jouzel, J. *Nature* **366,** 552–554 (1993).
6. Dansgaard, W. *et al. Science* **218,** 1273–1277 (1982).
7. Dansgaard, W. *et al.* in *Climate Processes and Climate Sensitivity* (eds Hansen, J. E. & Takahashi, T.) 288–298 (Geophys. Monogr. No. 29, Am. geophys. Un., Washington DC, 1984).
8. Dansgaard, W., White, J. W. C. & Johnson, S. J. *Nature* **339,** 532–534 (1989).
9. Broecker, W. S., Peteet, D. M. & Rind, D. *Nature* **315,** 21–26 (1985).
10. Broecker, W. S. *et al. Paleoceanography* **3,** 1–19 (1988).
11. Keigwin, L. A., Jones, G. A. & Lehman, S. J. *J. geophys. Res.* **96,** 16811–16826 (1991).
12. Dansgaard, W., Johnsen, S. J., Clausen, H. B. & Langway, C. C. in *The Late Cenozoic Glacial Ages* (ed. Turekian, K. K.) 37–56 (Yale Univ. Press, New Haven, 1971).
13. Hibler, W. D. & Johnsen, S. J. *Nature* **280,** 481–483 (1979).
14. Birchfield, G. E. & Broecker, W. S. *Paleoceanography* **5,** 835–843 (1990).
15. Broecker, W. S., Bond, G. & Klas, M. *Paleoceanography* **5,** 469–477 (1990).
16. Cox, M. D. *Tech. Rep.* No. 1 (*GFDL Ocean Group, Princeton University,* New Jersey, 1984).
17. Bryan, F. *J. phys. Oceanogr.* **17,** 970–985 (1987).
18. Levitus, S. *NOAA Prof. Pap. No. 13* (*US Department of Commerce, NOAA,* Rockville, 1982).
19. Weaver, A. J., Sarachik, E. S. & Marotzke, J. *Nature* **353,** 836–838 (1991).
20. Hughes, T. M. C. & Weaver, A. J. *J. phys. Oceanogr.* (in the press).
21. Weaver, A. J., Marotzke, J., Cummins, P. F. & Sarachik, E. S. *J. phys. Oceanogr.* **23,** 39–60 (1993).
22. Hasselmann, K. *Tellus* **28,** 473–485 (1976).
23. Mikolajewicz, U. & Maier-Reimer, E. *Clim. Dynam.* **4,** 145–156 (1990).
24. Baumgartner, A. & Reichel, E. *The World Water Balance* (Elsevier, New York, 1975).
25. Manabe, S. & Stouffer, R. J. *Nature* **364,** 215–218 (1993).
26. Stocker, T. F. & Wright, D. G. *Nature* **351,** 729–732 (1991).
27. Bryan, F. *Nature* **323,** 301–304 (1986).
28. Broecker, W. *Oceanography* **4,** 79–89 (1991).
29. Maier-Reimer, E. & Mikolajewicz, U. in *Oceanography* (eds Ayala-Castanares, A. *et al.*) 87–100 (UNAM Press, Mexico, 1989).

ACKNOWLEDGEMENTS. We thank the Canadian NSERC, AES and NSERC/WOCE for financial support (A.J.W.), and for an NSERC postgraduate fellowship (T.H.). We are grateful to the Canadian Climate Centre for providing us with computer time on their high-speed IBM workstation cluster.

The instability of a vaporization front in hot porous rock

Shaun D. Fitzgerald & Andrew W. Woods

Institute of Theoretical Geophysics,
Department of Applied Mathematics and Theoretical Physics,
Cambridge CB3 9EW, UK

In many geothermal systems, water migrates into vapour-dominated porous rock either through natural recharge or through forced injection of water from a well[1–5]. If the host rock is initially very hot, then a fraction of this injected water vaporizes[6,7]; as the water injection rate increases, the fraction which vaporizes decreases[7]. For modelling purposes, it is generally assumed that liquid–vapour interfaces in hot porous rocks are planar and stable[6,7]. But we show here, both theoretically and experimentally, that if a sufficient fraction of the liquid vaporizes, the interface can become unstable. The resulting 'fingering' instability can itself be stabilized: at short wavelengths by thermal diffusion, and at long wavelengths by the pressure increase caused by the excess vaporization at the tips of the fingers. These liquid fingers migrate through the porous rock much more rapidly than does a planar liquid front, and could therefore limit the time during which vapour may be extracted for geothermal power applications. We suggest that an optimal water injection rate for geothermal energy production may be that for which the interface is just stable, thereby maximizing the fraction of liquid which vaporizes, while suppressing the fingering instability.

High-temperature geothermal circulation systems involve complex liquid and vapour flow and phase change through permeable strata[1,8]. Determination of the rate of vapour production as liquid invades a reservoir is crucial for optimizing geothermal power generation[7,9,10], for geochemical monitoring of the mixing of different fluid masses[2,11], for monitoring volcanic activity[12] and for understanding aspects of ore deposition[13,14]. Vapour-dominated reservoirs, including the Geysers, California, are of particular interest because the extraction of vapour for power generation has led to a significant decline in the reservoir pressure and fluid levels[15,16]. New vapour may be generated as water invades the reservoir and is heated by the hot rock. It is commonly assumed that in geothermal systems, such liquid–vapour interfaces migrating into the vapour-saturated region are stable and planar[6,7]. This is motivated by the argument that a liquid finger advancing ahead of a liquid–vapour interface has a larger surface area exposed to the hot rock, vaporizes more rapidly, and is thus resorbed into the front[6]. Indeed, in reservoirs of very low permeability, static liquid–vapour interfaces are stable to disturbances, even if the liquid overlies the vapour[17]. Moreover, the classical result of Saffman–Taylor[18] shows that when a viscous fluid flows into a porous rock filled with a second fluid of lower dynamic viscosity, the interface remains stable and planar. In contrast, we show here that a migrating liquid–vapour interface may in fact become unstable.

The pressure gradient, G_l, in liquid of dynamic viscosity μ_l and density ρ_l which flows through a liquid-saturated porous rock of permeability K with Darcy velocity u_l is $G_l = -\mu_l u_l / K$ (ref. 8). Suppose that a mass fraction $f (0 \leqslant f \leqslant 1)$ of this liquid vaporizes and migrates ahead of the moving liquid–vapour interface. Then, by mass conservation, just ahead of the interface in the vapour-saturated region, this newly formed vapour has Darcy velocity $u_v = f u_l \rho_l / \rho_v$ and pressure gradient $G_v = -f \mu_v u_l \rho_l / K \rho_v$, where the vapour is of density ρ_v and dynamic viscosity μ_v. If the magnitude of the pressure gradient in the vapour exceeds that in the liquid, $|G_v| > |G_l|$, then, as with other migrating fluid–fluid interfaces[17,19], the interface can become

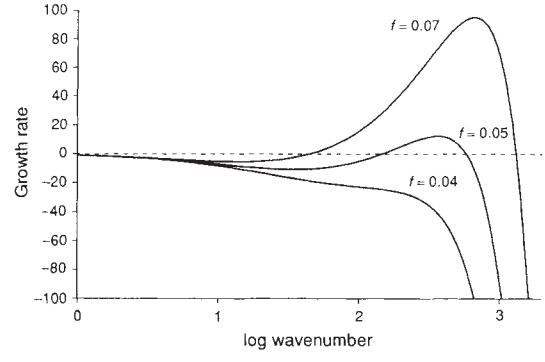

FIG. 1 Growth rate (σ) of a perturbation as a function of the wavenumber (k). Curves are given for three values of the mass fraction vaporizing (f). In these calculations the thermal diffusivity $\kappa = 3 \times 10^{-6}$, $\kappa/\alpha = 5 \times 10^{-4}$ and $\nu_l/\nu_v = 0.042$. Note that Woods and Fitzgerald[7] have shown that f lies in the range $0 < f < 0.8$ for injection of liquid water in a cylindrical geometry, with the value of f decreasing with injection rate, and that typically $\nu_l/\nu_v \approx 0.1$–0.2 in vapour-dominated geothermal reservoirs[20].